

## Robust Model Reference Fault Detection and Identification System for Fixed Wing Aircrafts

R. Jaganraj<sup>a</sup> and R. Velu

Vel Tech Rangarajan Dr. Sagunthala R&D Institute of Science and Technology, Chennai, India

<sup>a</sup>Corresponding Author, Email: [ravishankarjaganraj@gmail.com](mailto:ravishankarjaganraj@gmail.com)

### ABSTRACT:

Fault Detection and Identification system (FDI) and Fault Tolerant Flight Control (FTFC) system are used to correct the faulty operation of an aircraft. Both FDI and FTFCs have operational disadvantages due to their inherent limitation of fault source identification. This paper presents the design and implementation of a robust model reference fault detection and identification (MRFDI) system on a fixed-wing aircraft for identifying actuator fault, instrument fault and presence of any uncertainties. The proposed MRFDI fuses the real-time parameters and actuator feedback to combine the advantages of data driven and model reference FDI that makes robust fault estimation. The MRFDI system is implemented on a typical aircraft altitude hold autopilot simulation environment with a predefined fault scenario. The fault scenario includes a faulty elevator, a faulty skin-implantable sensor and wind gust as environmental uncertainty. The MRFDI performs logical analysis to detect fault using state-dependent real-time parameters and state-independent skin implantable sensor. This two-step fault detection method makes MRFDI robust to any type of fault identification. The results show that the MRFDI detects and distinguishes faults in actuator, instrument and any of the listed uncertainties thrown by the environment accurately.

### KEYWORDS:

Model reference fault detection and identification system; Real-time system identification; Autopilot

### CITATION:

R. Jaganraj and R. Velu. 2018. Robust Model Reference Fault Detection and Identification System for Fixed Wing Aircrafts, *Int. J. Vehicle Structures & Systems*, 10(5), 371-376. doi:10.4273/ijvss.10.5.14.

### ACRONYMS AND NOMENCLATURE:

$v_x$	velocity- x direction in m/s
$v_y$	velocity- y direction in m/s
$q$	pitch rate in rad/s
$\theta$	pitch angle in rad
$\delta_e$	elevator deflection in rad
$\delta_t$	throttle input in rad

## 1. Introduction

Fault-tolerant flight control (FTFC) and Fault detection and identification (FDI) are the most active research areas today. FTFC is applied on an autopilot system for successful resuming of aircraft operation after malfunctions. Faults or failures are defined as deviation in any one/more performance characteristics of the system to the corresponding input. FDI is used in FTFC for suitable corrective measures to prevent the system from further deviation which may lead to failure. FTFC takes corrective measures without implementation of FDI by estimating the deviation in demanded and attained aircraft performance.

Most of the FTFC are functioning without FDI and employ a combination of different control methods. FTFC is experimented on twin-engine small aircraft (without implementation of FDI on-board) to recover faulty behaviour of aircraft by comparing variation in demanded and achieved attitude of aircraft [1]. FTFC generates suitable guidance commands using inner loop (acceleration data) and outer loop (attitude data)

feedback controller. The fault scenario executed includes propulsion only mission (all actuators failure), loss of 25% and 50% wing during mid-flight and injected time delay. They successfully demonstrated the operation of FTFC within conservative altitude limit. It was also explained that the absence of FDI limits the functionality of FTFC due to a conservative altitude limit. Further, it was also suggested that if the FDI was implemented within the system, FTFC would overcome this limitation. The system identification of a damaged aircraft was demonstrated using wind tunnel experiments and by real flight tests [2] and [3]. They also explained that the method was based on the reallocation of dynamical model of normal flight condition to faulty condition during the corresponding fault.

Trimmable Horizontal Surface (THS) was developed to demonstrate FTFC on a commercial aircraft model [4]. The assumptions made were that the elevator equipped with another small elevator surface (trim) and fault scenario as the malfunction in main elevator actuator. They assumed feedback of actuator to be an FDI. Also, presence of the uncertainty was not considered. Similar work was carried out with the presence of uncertain environment as wind gust [5]. They equipped their model with twin actuator configuration (primary elevator and secondary trim control in elevator). The uncertainty and disturbance estimator (UDE) was applied on FTFC based on nonlinear dynamic inversion. The control would be

reallocated to secondary actuator during malfunction of primary control. They also assumed that the opposite of estimated disturbance could be used in FTFC to nullify the effect of disturbance. Further, they tested their system for wind gust uncertain condition (without actuator fault) by assuming healthy operation of primary control. However, the source of the fault was unaddressed and limited for instrument error. They also explained that the system assumed deviation in performance as the environmental uncertainty, if the fault was not found in primary actuator.

FTFC is classified into active and passive control [6] and [7]. The passive FTFC requires fault detection, identification and control reconfiguration, whereas, the active method reacts to demands (faults) actively by reconfigurable control scheme. Various mathematical models and approaches for reconfiguration techniques were also discussed broadly. The fusion of Linear Quadratic Regulator (LQR) and Model Reference Adaptive Control (MARC) are applied on dissimilar redundant actuation system for flight control during faulty scenario [8]. This system used damaged aircraft dynamic model as control strategy. Research works were carried out for identifying dynamics of aircraft with structural failure. The aircraft stability was analysed for nonlinear region and equilibrium point was determined for icing condition and normal condition [9]. The simulated aircraft attributes (angle of attack, sideslip, roll rate, pitch rate and yaw rate) were modelled as functions of elevator deflection. These attributes were compared for normal flight and icing flight condition. The variation in geometry of aircraft influenced in change of equilibrium point and the observations were presented.

The controllability analysis of tandem quad-copter was carried out [10]. The adaptive control algorithm with actuator saturation is applied on numerical simulation. FDI scheme was developed to estimate fault using comparison of required attitude to the measured attitude [11]. The fault detection of air data sensor is developed by sensor fusion [12]. They estimated the fault based on comparison of state variables to identify sensor fault and it is robust to some extent, because of comparing state of air data sensor output to the aircraft response for detecting instrument only fault. So, the robust estimator requires real time parameter estimator and state-independent actuator/sensor feedback. The real-time parameters of aerodynamic model were estimated using artificial intelligence [13]. The method of system identification was explained briefly for a small unmanned aircraft [14]. The real-time parameter estimation of aircraft was carried out using recursive least square and batch estimation method [15] and minimized error in each model. System identification using subscale methods were explained for small flexible aircraft [16].

Many of the work done so far on FTFC focused on control reallocation to healthy components, employing additional secondary actuator and improving accuracy in FTFC. However, these methods are limited due to corresponding control saturation and challenge during the presence of any uncertainties in the operational environment or in a catastrophic failure. These situations include instrument measurement error, dynamical

instability due to uneven wind pattern, control effectiveness and structural failure.

FDI methods were operated by either data-driven or model reference approach for diagnosing fault [20]. Data-driven models use supervising of components, signals and processes. Model reference system uses the comparison of desired to the attained performance of the actual model and reference model. So far, FTFC has been implemented in two ways (1) Control reallocation with FDI and (2) Control by nullifying errors using proper control reallocation/corrective measures. FDI has been implemented by comparing input to the output or estimating error in actuator feedback. Most of the FDI and FTFCs have inherent limitation in inadequate identification of actual source of malfunction. The robustness of FDI will improve the detection of fault and its source to overcome limitations of FTFC. Implementation of FDI scheme is required for the effective application of FTFC without any inherent chaos in control logic [1] and [3].

Many of the FDI methods use comparison of feedback of input with corresponding aircraft output to identify fault. However, both FTFC and FDI methods have a marked disadvantage due to their inherent failure in inadequate estimation of fault and its source. These methods have only considered variation in demanded output to the actual output and have monitored actuator health. These methods become ineffective when FTFC undergoes logical ambiguity during the presence of uncertainties. These uncertainties may happen even if aircraft has fully functional actuators and instruments. Hence a FTFC system does not serve well during uncertain operating conditions. These operating conditions make the FTFC to take faulty decision during reallocation of control or implementing corrective measures. Therefore, limitations of FTFC lie in improper estimation of a fault and its source.

Present work is based on the motivation to overcome the limitations in FDI by developing a robust Model Reference Fault Detection and Identification (MRFDI) system to detect any fault and identify its source. The MRFDI uses skin implantable sensors to detect input uncertainty (actuator fault) followed by the logical identification of a source using sequential parameter estimation. Robust fault detection requires both state-dependent variables of an aircraft and state-independent feedback of actuators so as to identify the fault source. The uncertainty in the environment influences directly on the dynamics and corresponding response of an aircraft. The MRFDI detects the fault followed by identification of its source with robust two-step verification. Subsequently, MRFDI is successfully implemented on simulated aircraft dynamics for the robust detection of actuator fault, instrument fault and any instability in environment.

Present study aims to develop MRFDI to detect and identify a fault and its origin to understand the behaviour of the system. This includes presence of any uncertainty thrown by the environment. MRFDI improves the redundancy in fault detection in all faulty situations include actuator fault, measurement fault and uncertain environment. FDI scheme is developed with two-step verification logic consist of comparison of state-

dependent and state-independent aircraft attributes and hence considered to be robust. The MRFDI is applied on simulated altitude hold autopilot system. The real time parameter estimation is validated by base model parameters. The actuator feedback and parameters are analysed by MRDFI logic and a fault and its source are successfully identified.

## 2. Aircraft system identification

A longitudinal linearized aircraft mathematical model [17] is given by,

$$\dot{x} = Ax + Bu \quad (1)$$

$$y = Cx + Du \quad (2)$$

Where  $\dot{x} = [\dot{v}_x \dot{v}_z \dot{q} \dot{\theta}]^T$ ,  $x = [v_x v_z q \theta]^T$  and  $u = [\delta_e \delta_t]^T$ .  $x$  and  $\dot{x}$  are the velocity, acceleration response of the aircraft and  $u$  is the control input.  $\dot{v}_x, \dot{v}_z, \dot{q}, \dot{\theta}$  are acceleration in direction x, direction z, rate of pitch rate and rate of pitch angle respectively.  $v_x, v_z, q, \theta$  are velocity in direction x, direction z, pitch rate and pitch angle.  $\delta_e, \delta_t$  are the elevator and throttle control input. A and B are the unknown parameters of stability and control derivatives of the aircraft. D and C are the output matrices. System identification technique is used to estimate the unknown parameters. Typical B747 aircraft parameters (values of A and B) are applied on Eqns. (1) and (2). An altitude hold autopilot is developed to simulate longitudinal altitude hold autopilot system [18]. The altitude hold autopilot system is shown in Fig. 1.

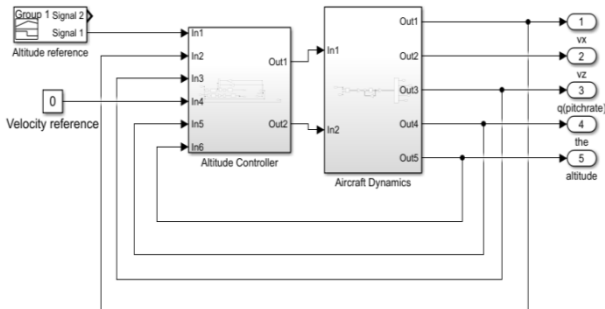


**Fig. 1: Altitude hold autopilot for system identification of aircraft**

The altitude reference value is given as 475m from 50s to 250s and 750m from 300s to 500s. The altitude hold autopilot estimates required correction for elevator and throttle to maintain the given reference altitude and velocity. This estimation is using the feedback from the aircraft altitude and velocity. The pitch and altitude controller generates the corresponding elevator and throttle commands to compensate the altitude and velocity correction. Fig. 2 shows the results of the autopilot system. Fig. 2(a) shows the velocity ( $v_x$ ), the angle of attack ( $\alpha$ ) and pitch angle ( $\theta$ ). The results shown in Fig. 2(b) explain that the aircraft is following the reference path given to the autopilot. Fig. 2(c) shows that the autopilot system generates input commands of an elevator ( $\delta_e$ ) and throttle ( $\delta_t$ ). Mathematical approaches for system identification problem are well established [20]. One of the simplest and reliable approaches is the least square (LS) method [16].

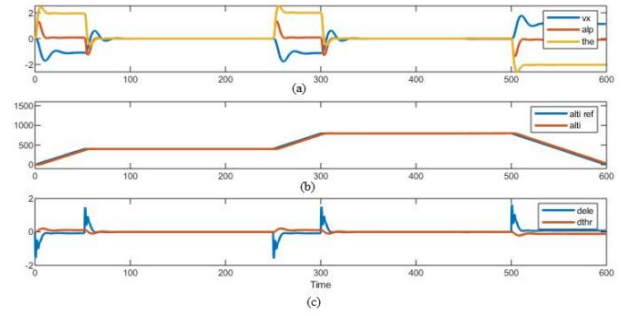


**Fig. 2: Flight path of altitude hold system**

The simulated inputs and outputs are given by,

$$x = [v_x v_z q \theta]^T \quad Y = \phi X \quad (3)$$

$$J = \frac{1}{2} (Y - \phi X)^T (Y - \phi X) \quad (4)$$

$$\phi = (YX^T) (X^T X)^{-1} \quad (5)$$

Where  $Y$  is the output of the system and  $X$  is the input of the system. The unknown parameters are  $\phi$  and it can be estimated from Eqn. (5) using LS method. The inputs of  $X$  are  $\dot{x} = [\dot{v}_x \dot{v}_z \dot{q} \dot{\theta}]^T$  and outputs of  $Y$  are

$J$  in Eqn. 4 is the cost function of errors. To minimize the cost function, the gradient is equated to zero resulting in Eqn. (5). The parameters A and B are estimated by LS method for B747. The estimated parameters are compared with base line parameters of B747. The values of B747 base line parameters (base) and simulated parameters (LS) are given in Table 1.

**Table 1: Comparison of baseline parameter with estimated (LS) parameters of A**

		Base	-0.00687	0.01394	0	-9.81
$A_{1j}$	Base	-0.00687	0.01394	0	-9.81	
	LS	-0.00687	0.01394	0	-9.81	
$A_{2j}$	Base	-0.09050	-0.31491	235	0	
	LS	-0.09050	-0.31491	235	0	
$A_{3j}$	Base	0.00039	-0.00336	-0.428	0	
	LS	0.00039	-0.00336	-0.428	0	
$A_{4j}$	Base	0.00000	0.00000	1	0	
	LS	0.00000	0.00000	1	0	

The base parameter estimation model is then converted into sequential parameter estimation by,

$$\phi_{N+1} = (Y_{N+1} X_{N+1}^T) (X_{N+1}^T X_{N+1})^{-1} \quad (6)$$

Where  $N$  denotes the  $N^{\text{th}}$  second of experiment data [15]. This sequential identification simultaneously adds new experiment data to the existing experiment data of  $\dot{x}$ ,  $x$  are given by,

$$X_{N+1} = [x_N \quad x_{N+1}] \quad (7)$$

$$Y_{N+1} = [y_N \quad y_{N+1}] \quad (8)$$

The simulated inputs and outputs are applied on this sequential least square (SLS) estimator and parameters are obtained for each experimented data. To validate the convergence of parameters, values of  $A_{b11}$  (first element of matrix A - base line model) and  $A_{11}$  (first element of actual model matrix A) are given in Table 2. The parameters are converged with initial error as the sacrifice to achieve real time parameter [15]. The results

are analysed for time taken to attain steady state. Fig. 3(a) shows that the steady state is attained after 3s.

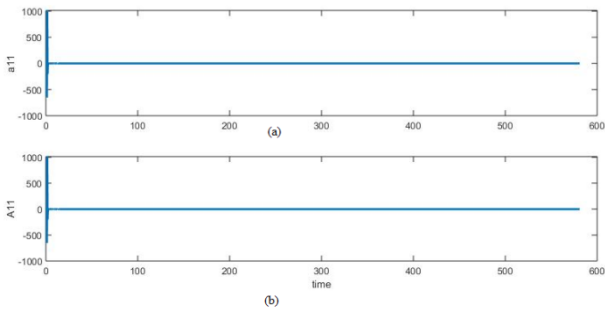


Fig. 3: Flight convergence of parameters (SLS)

Table 2: Comparison of baseline parameter with sequential LS before and after 3s

Base line ( $A_{b11}$ )	LS ( $A_{11}$ )	SLS (before 3s, $A_{11}$ )	SLS (after 3s, $A_{11}$ )
-0.00687	-0.00687	0.23428	-0.00687

### 3. Development of MRFDI

MRFDI is developed by cloning the autopilot model. The base autopilot model block modified by adding reference model block as shown in Fig. 4. The actual model is assumed to be a real aircraft and the reference model to be a mathematical model of real aircraft. Generally, this model reference approach is used as a control scheme in FTFC. This study utilizes this model reference for FDI. The altitude and velocity reference command are common for both actual and reference model. To simulate the fault, predefined actuator fault (in this case elevator) is injected during mid-flight to the actual model from 350s to 360s as constant increment with actuator input as shown Fig. 5.

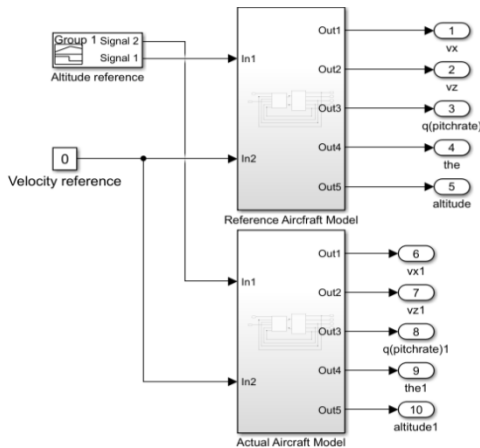


Fig. 4: Model reference system

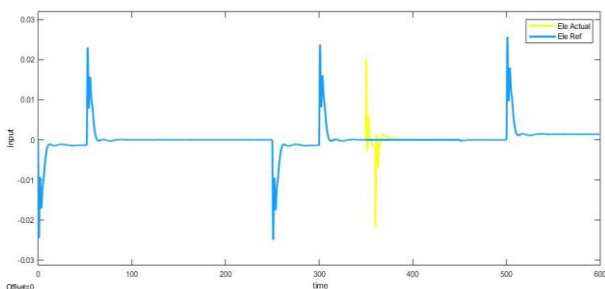


Fig. 5: Elevator input with fault injection

To identify fault in actuator, skin implantable sensor is modelled as feedback of actual model elevator input. In real time, skin implantable sensor measures actuator, output and transmit data as feedback of actuator. The influence of fault injection on actual model is shown in Fig. 6. As the error enters into the actual system during mid-flight, the results show that aircraft altitude deviates from reference altitude. The SLS method is applied on actual model and reference model to get parameters. The identified parameter convergence of  $a_{11}$  (actual model) and  $A_{11}$  (reference model) is shown in Fig. 3.

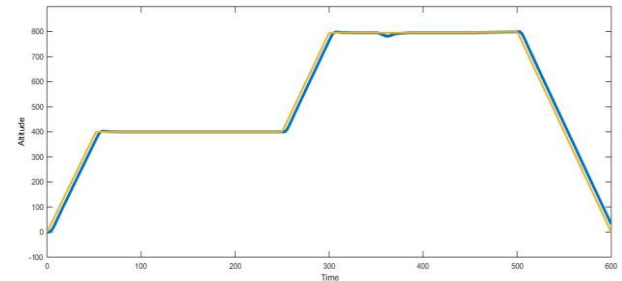


Fig. 6: Flight path variation with faulty elevator at 350s

### 4. FDI framework

The fault detection and identification scheme used in MRFDI framework logically analyses the actuator feedback and parameters of actual and reference model. The model similarity in actual and reference model is used to develop fundamental architecture of MRFDI. The developed MRFDI system is shown in Fig. 7 and its logical scheme is given in Table 3.

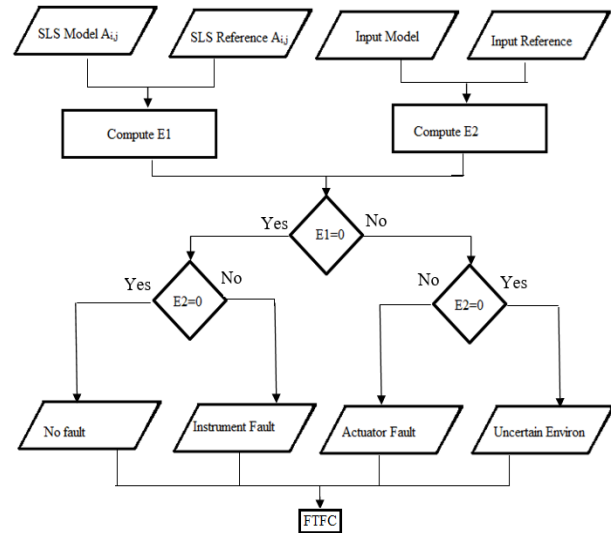


Fig. 7: Model reference FDI

The MRFDI consists of skin implantable sensor to detect fault in actuator. This sensor measures the actual deflection of control surface to the corresponding control input. In this work, the skin implantable sensor is modelled as feedback of elevator input. This feedback system works as virtual skin implantable sensor to supervise control input to the actual model. The MRFDI compares the parameters of actual model with reference model parameters and shows error flag value as 1, if any variation found in parameters. Similarly virtual skin implantable sensor error flag value as 1, if any variation

found in actuator input. MRFDI logically check the flag values of parameter error and actuator error as given in Table 3. The detection and identification follow the logic in Table 3 for robust estimation of fault and its source.

**Table 3: MRFDI scheme for robust fault tolerant**

Skin implantable sensor	Variation in actual and reference parameter	Actuator fault	Instrument fault	Environ. uncertainty
1	0	0	1	0
1	1	1	0	0
0	1	0	0	1
0	0	0	0	0

**5. Results and discussions**

The following fault scenarios were simulated using MRFDI system:

- Case 1 - Elevator fault during 350s of flight
- Case 2 - Virtual skin implantable instrument fault during 350s
- Case 3 - Wind gust during 350s

For Case 1, the actual model input is added to the constant increment to simulate the error during 350s. SLS method was employed on actual and reference model to get real time parameters. The actuator feedback and real time parameters were analysed by MRFDI fault detection algorithm using the values given in Table 3. Fig. 8 shows the comparison made by MRFDI. It verifies the parameter  $a_{11}$  and  $A_{11}$  of actual model and reference model to estimate error in parameters as shown in Figs. 8(a) and 8(b). The variation of parameters shown in Fig. 8(c) confirms that the fault occurred during 350s.

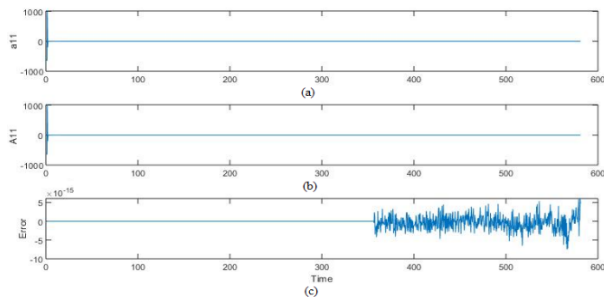


**Fig. 8: Comparison of parameters of actual and reference model**

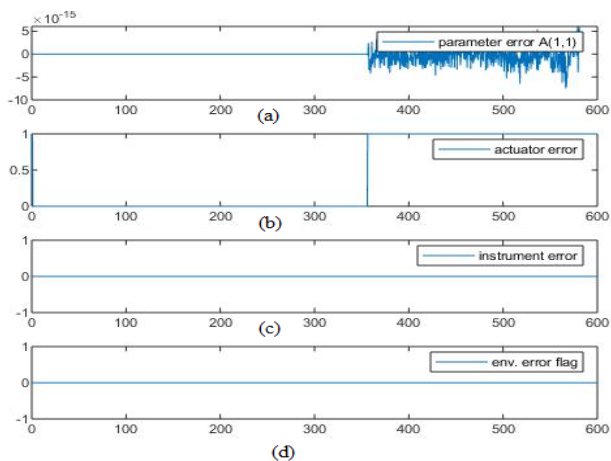


**Fig. 9: Case 1 - Estimation of actuator fault**

The MRFDI verifies the logic given in Table 3 and estimates a fault as flag value '1' as shown in Fig. 9. The skin implantable sensor output of actual model detects the actuator failure during 350s of the flight. Finally MRFDI estimates a fault source as actuator error. The MRFDI fault detection result for Case 1 simulation is shown in Fig. 9. The MRFDI detects the parameter variation as shown in Fig. 9(a) and then a source as actuator fault as shown in Fig. 9(b). Fig. 9(c) and 9(d) show that the fault is not occurred due to instrumental fault and uncertain environmental effect.

For Case 2, the error is simulated by adding constant increment error to virtual skin implantable sensor (actuator feedback) during 350s. Like Case 1, Case 2 also begins with comparison of parameters followed by error flag estimation using Table 3 logic. The results are shown in Fig. 10 for Case 2 simulation. Since the error is injected only at virtual skin implantable sensor, the MRFDI detects no variation in parameters as shown in Fig. 10(a). Fig. 10(b) shows that the MRFDI detects actuator fault and identifies that the actual reason for error as instrument fault as shown in Fig. 10(c). 10(d) shows that the fault was not occurred due to uncertainty.

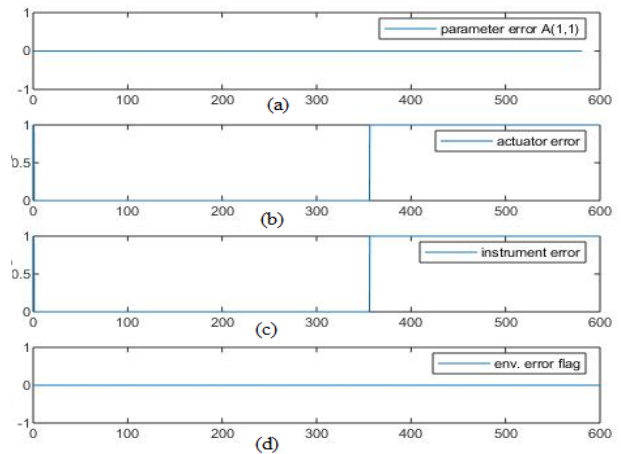


**Fig. 10: Case 2 - estimation of instrument fault**

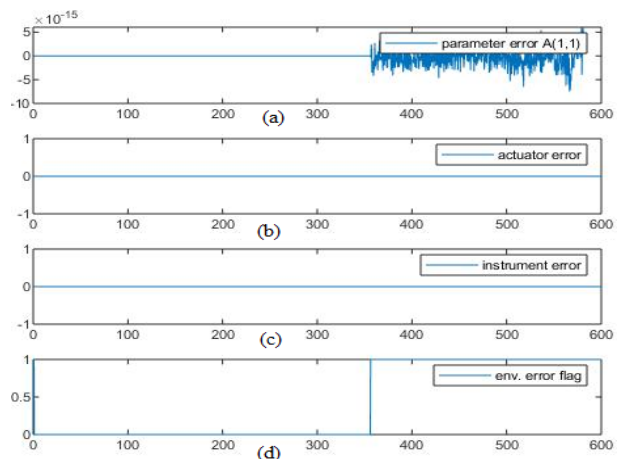


**Fig. 11: Case 3 - Estimation of dynamical instability / identification of catastrophic failure**

For Case 3, the error is simulated by adding a constant increment with velocity during 350s as a wind gust. Since no error has occurred at actuator and actuator feedback system, Fig. 11(b) and 11(c) show no variation in actuator and actuator feedback. Fig. 11(a) shows a

variation in parameters. Fig. 11(d) shows the presence of an uncertain environment. The results of Case 3 confirm that the fault occurred due to a wind gust and reflections are observed only at parameters.

## 6. Conclusion

An MRFDI scheme is developed to identify and distinguish the nature of fault. A typical aircraft mathematical model is developed along with altitude hold autopilot for applying MRFDI. The estimated parameters are validated using least square and sequential least square method. The developed MRFDI demonstrated the capability to successfully detect and identify the fault along with its source for a predefined scenario, in a simulated environment. The results also confirmed that the developed MRFDI is robust in nature and capable of identifying actuator fault, instrument fault and dynamic instability. Coupled with an MRFDI for fault tolerant flight control, MRFDI will prove a potential system in flight operation and control.

## REFERENCES:

- [1] G. Chowdhary, E.N. Johnson, R. Chandramohan, M.S. Kimbrell and A. Calise. 2013. Guidance and control of airplanes under actuator failures and severe structural damage, *J. Guidance, Control, and Dynamics*, 36(4), 1093-1104. <https://doi.org/10.2514/1.58028>.
- [2] G. Chowdhary, W.D. Busk and E. Johnson. 2010. Real-time system identification of a small multi-engine aircraft with structural damage, *AIAA Paper 2010-3472*. <https://doi.org/10.2514/6.2010-3472>.
- [3] D. Jourdan, M. Piedmonte, V. Gavrillets, D. Vos and J.M. Cormick. 2010. Enhancing UAV survivability through damage tolerant control, *Proc. AIAA Guidance, Navigation, and Control Conf.*, Toronto, Canada. <https://doi.org/10.2514/6.2010-7548>.
- [4] X. Wang, S. Wang, Z. Yang and C. Zhang. 2015. Active fault-tolerant control strategy of large civil aircraft under elevator failures, *Chinese J. Aeronautics*, 28(6), 1658-1666. <https://doi.org/10.1016/j.cja.2015.10.001>.
- [5] D.D. Dhadekar and S.E. Talole. 2018. Robust fault tolerant longitudinal aircraft control, *IFAC-Papers on Line*, 51(1), 604-609. <https://doi.org/10.1016/j.ifacol.2018.05.101>.
- [6] Y. Zhang and J. Jiang. 2003. Bibliographical review on reconfigurable fault-tolerant control systems, *Proc. 5th IFAC Symp. Fault Detection, Supervision and Safety for Technical Processes*, 265-276. [https://doi.org/10.1016/S1474-6670\(17\)36503-5](https://doi.org/10.1016/S1474-6670(17)36503-5).
- [7] X. Yu and Y. Zhang. 2015. Design of passive fault-tolerant flight controller against actuator failures, *Chinese J. Aeronautics*, 28(1), 180-190. <https://doi.org/10.1016/j.cja.2014.12.006>.
- [8] J. Wang, S. Wang, X. Wang, C. Shi and M.M. Tomovic. 2016. Active fault tolerant control for vertical tail damaged aircraft with dissimilar redundant actuation system, *Chinese J. Aeronautics*, 29(5), 1313-1325. <https://doi.org/10.1016/j.cja.2016.08.009>.
- [9] Q.U. Liang, L.I. Yinghui, X.U. Haojun, D. Zhang and Y.U.A.N. Guoqiang. 2017. Aircraft nonlinear stability analysis and multidimensional stability region estimation under icing conditions, *Chinese J. Aeronautics*, 30(3), 976-982. <https://doi.org/10.1016/j.cja.2017.02.003>.
- [10] X. Wang, C. Xiang, H. Najjaran, B. Xu. 2018. Robust adaptive fault-tolerant control of a tandem coaxial ducted fan aircraft with actuator saturation, *Chinese J. Aeronautics*, 31(6), 1298-1310. <https://doi.org/10.1016/j.cja.2018.03.018>.
- [11] R. Khan, P. Williams, P. Riseborough, A. Rao and R. Hill. 2016. Active fault tolerant flight control system design, *arXiv:1610.02139v1*, 1-31.
- [12] O.N. Korsun, M.H. Om, K.Z. Latt and A.V. Stulovskii. 2017. Real-time aerodynamic parameter identification for the purpose of aircraft intelligent technical state monitoring, *Proc. Computer Sci.*, 103, 67-74. <https://doi.org/10.1016/j.procs.2017.01.014>.
- [13] O.N. Korsun, B.K. Poplavsky and S.J. Prihodko. 2017. Intelligent support for aircraft flight test data processing in problem of engine thrust estimation, *Proc. Computer Sci.*, 103, 82-87. <https://doi.org/10.1016/j.procs.2017.01.017>.
- [14] A. Dorobantu, A. Murch, B. Mettler and G. Balas. 2013. System identification for small, low-cost, fixed-wing unmanned aircraft, *J. Aircraft*, 50(4), 1117-1130. <https://doi.org/10.2514/1.C032065>.
- [15] J.A. Grauer. 2016. Parameter uncertainty for aircraft aerodynamic modeling using recursive least squares, *Proc. AIAA Atmospheric Flight Mechanics Conf.*, San Diego, California, USA. <https://doi.org/10.2514/6.2016-2009>.
- [16] H. Pfifer and B.P. Danowsky. 2016. System Identification of a small flexible aircraft-invited, *Proc. AIAA Atmospheric Flight Mechanics Conf.*, San Diego, California, USA. <https://doi.org/10.2514/6.2016-1750>.
- [17] R.C. Nelson. 1989. *Flight Stability and Automatic Control*, McGraw-Hill, New York.
- [18] B. Etkin and L.D. Reid. 1996. *Dynamics of Flight: Stability and Control*, 3<sup>rd</sup> Ed., New York.
- [19] R.V. Jategaonkar. 2015. *Flight Vehicle System Identification: A Time-Domain Methodology*, AIAA. <https://doi.org/10.2514/4.102790>.
- [20] N. Bayar, S. Darmoul, S.H. Gabouj and H. Pierreval. 2015. Fault detection, diagnosis and recovery using artificial immune systems: A review, *Engg. Applications of Artificial Intelligence*, 46, 43-57. <https://doi.org/10.1016/j.engappai.2015.08.006>.